

# EXTENDING DIFFERENTIAL TEMPORAL DIFFERENCE METHODS FOR EPISODIC PROBLEMS

000  
001  
002  
003  
004  
005 **Anonymous authors**  
006 Paper under double-blind review  
007  
008  
009  
010

## ABSTRACT

011 Differential temporal difference (TD) methods are value-based reinforcement  
012 learning algorithms that have been proposed for infinite-horizon problems. They  
013 rely on reward centering, where each reward is centered by the average reward.  
014 This keeps the return bounded and removes a value function’s state-independent  
015 offset. However, reward centering can alter the optimal policy in episodic prob-  
016 lems, limiting its applicability. Motivated by recent works that emphasize the role  
017 of normalization in streaming deep reinforcement learning, we study reward cen-  
018 tering in episodic problems and propose a generalization of differential TD. We  
019 prove that this generalization maintains the ordering of policies in the presence  
020 of termination, and thus extends differential TD to episodic problems. We show  
021 equivalence with a form of linear TD, thereby inheriting theoretical guarantees  
022 that have been shown for those algorithms. We then extend several streaming re-  
023inforcement learning algorithms to their differential counterparts. Across a range  
024 of base algorithms and environments, we empirically validate that reward center-  
025 ing can improve sample efficiency in episodic problems.  
026

## 1 INTRODUCTION

027 The average reward formulation of reinforcement learning (Mahadevan, 1996)—which can be de-  
028 scribed as an undiscounted objective for continuing problems—has led to the development of algo-  
029 rithms that shift rewards by the average reward (Schwartz, 1993; Sutton & Barto, 2018; Wan et al.,  
030 2021). This mean-centering of rewards prevents the undiscounted, infinite sum of rewards from  
031 diverging. Temporal difference (TD) methods which predict this sum of centered rewards form the  
032 *differential* TD family of algorithms. Recent work separated centering from the average reward  
033 formulation by demonstrating its utility in discounted problems (Naik et al., 2024; Naik, 2024)—a  
034 setting where centering is not necessary for bounding an infinite sum of rewards. However, its use  
035 remains limited to continuing problems because in episodic problems, the ordering of policies is not  
036 preserved when rewards are shifted. To illustrate this, consider an episodic problem where some  
037 positive constant  $c$  is subtracted from every reward. Subtracting a sufficiently large  $c$  produces op-  
038 timal behavior which terminates as quickly as possible. Conversely, adding a sufficiently large  $c$  to  
039 every reward encourages behavior that prolongs the episode (i.e., avoids termination).  
040

041 Normalization methods have recently garnered interest in deep reinforcement learning (e.g., Lyle  
042 et al., 2023; Lyle et al., 2024; Palenicek et al., 2025). Notably, normalization has shown substantial  
043 benefit in *streaming* deep reinforcement learning (Vassan et al., 2024; Elsayed et al., 2024)—the  
044 buffer-free, online, incremental learning setup of the original reinforcement learning algorithms  
045 (Sutton, 1988b; Sutton & Barto, 2018). Much of the recent work on normalization has focused on  
046 techniques such as input centering and scaling (Sutton, 1988a), layer normalization (Ba et al., 2016),  
047 and output scaling. However, less attention has been paid to output centering, with the lack of opti-  
048 mal policy invariance in episodic problems cited as the concern with it (Lee et al., 2025). Episodic  
049 environments are widely used for evaluation (e.g., Young & Tian, 2019; Towers et al., 2024), moti-  
050 vating a revisit of differential TD and exploring whether its applicability can be expanded.

051 In this work, we introduce a strict generalization of differential TD that extends its applicability to  
052 both discounted and undiscounted episodic problems. Through the lens of potential-based reward  
053 shaping, we prove that the modification maintains invariance of the optimal policies. We further  
show an equivalence between differential TD and a state-and-action-independent, output-level bias

054 unit, establishing that the algorithm shares theoretical guarantees (e.g., convergence to the fixed  
 055 point) with those of TD with linear function approximation. In tabular episodic problems, we high-  
 056 light the utility of centering and identify scenarios where we might expect improvement. Finally,  
 057 in the streaming deep reinforcement learning setting, we show that our generalization of differential  
 058 TD integrates seamlessly into existing algorithms, scales effectively to non-linear function approxi-  
 059 mation, and preserves the sample complexity benefits previously observed in continuing problems.  
 060

## 061 2 BACKGROUND AND RELATED WORK

063 Reinforcement learning is typically formalized as a Markov decision process (MDP), characterized  
 064 by a set of states  $\mathcal{S}$ , sets of each state's available actions  $\mathcal{A}(s)$ , and an environment transition model  
 065  $p(s', r|s, a) = P(S_{t+1} = s', R_{t+1} = r|S_t = s, A_t = a)$ . For each discrete time step  $t$ , an agent  
 066 observes its current state  $S_t \in \mathcal{S}$ , selects an action  $A_t \in \mathcal{A}(S_t)$ , and jointly samples a next state  
 067  $S_{t+1} \in \mathcal{S}$  and reward  $R_{t+1} \in \mathbb{R}$  according to the environment transition model. Actions are selected  
 068 according to a policy  $\pi(a|s) = P(A_t = a|S_t = s)$ , and reinforcement learning agents in control  
 069 problems aim to find the optimal policy  $\pi^*$  which maximizes a reward-based objective. A common  
 070 objective is to maximize the expected discounted return. The return is given by:

$$071 \quad G_t \stackrel{\text{def}}{=} \sum_{k=0}^{T-t-1} \gamma^k R_{t+k+1},$$

074 where  $\gamma \in [0, 1]$  and  $T$  being an episode's final time-step, or  $\gamma \in [0, 1)$  and  $T = \infty$  in infinite-  
 075 horizon, continuing problems. Value-based methods for reinforcement learning compute or approxi-  
 076 mate *value-functions*, which are defined to be expected returns conditioned on a state (or state-action  
 077 pair) under a policy  $\pi$ :

$$078 \quad v_\pi(s) \stackrel{\text{def}}{=} \mathbb{E}_\pi[G_t|S_t = s], \forall s$$

$$079 \quad q_\pi(s, a) \stackrel{\text{def}}{=} \mathbb{E}_\pi[G_t|S_t = s, A_t = a], \forall s, a,$$

081 with  $v_\pi(s)$  denoted the *state-value* function and  $q_\pi(s, a)$  denoted the *action-value* function. The  
 082 process of computing a policy's value function is referred to as *policy evaluation*. Such values may  
 083 then inform decisions via *policy improvement*—a theorem stating that behaving greedily with respect  
 084 to  $q_\pi$  will result in an improved policy  $\pi'$  where  $q_{\pi'}(s, a) \geq q_\pi(s, a), \forall s, a$ . Policy evaluation and  
 085 improvement can then alternate in a process of *policy iteration* to approach an optimal policy.

086 A popular approach to policy evaluation makes use of a value-function's Bellman equation, where a  
 087 decision point's value is expressed in terms of successor decision point values. For example, for  $v_\pi$ :

$$089 \quad v_\pi(s) = \sum_a \pi(a|s) \sum_{s', r} p(s', r|s, a) (r + \gamma v_\pi(s')), \forall s.$$

091 Given a transition  $(S_t, A_t, R_{t+1}, S_{t+1})$ , temporal difference (TD) methods (Sutton, 1988b) form a  
 092 sample-based estimate of  $v_\pi(S_t)$  based on its Bellman equation and take a step toward this target:

$$093 \quad V(S_t) \leftarrow V(S_t) + \alpha(R_{t+1} + \gamma V(S_{t+1}) - V(S_t)),$$

095 where  $V \approx v_\pi$  is a learned, approximate value function and  $\alpha \in [0, 1]$  is the step-size.

096 An alternative to the discounted objective is the average reward criterion (Mahadevan, 1996), where  
 097 an agent seeks to maximize its reward per step from some starting state  $S_0$ :

$$099 \quad r(\pi, s) \stackrel{\text{def}}{=} \lim_{n \rightarrow \infty} \frac{1}{n} \sum_{t=1}^n \mathbb{E}[R_t|S_0 = s, A_{0:t-1} \sim \pi], \forall s, \pi.$$

101 A unichain assumption is typically made on the MDP, making  $r(\pi, s)$  independent of state and  
 102 simplifying our notation to  $r(\pi)$ . This objective is akin to maximizing an undiscounted return in  
 103 an infinite-horizon, continuing setting. Standard value-based methods are not applicable here as  
 104 undiscounted, infinite-horizon returns are generally infinite. Value-based, average reward algorithms  
 105 instead work with *differential* returns:

$$106 \quad G_t^\Delta \stackrel{\text{def}}{=} \sum_{k=0}^{\infty} (R_{t+k+1} - r(\pi)),$$

108 where the average reward is subtracted from each reward to ensure the sum converges. Given cor-  
 109 responding differential value functions (e.g.,  $v_\pi^\Delta(s) \stackrel{\text{def}}{=} \mathbb{E}_\pi[G_t^\Delta | S_t = s]$ ), a TD method for this  
 110 setting maintains an estimate of its average reward (which we denote  $b$ ) and uses this to estimate the  
 111 differential return:

$$\begin{aligned} 112 \quad b &\leftarrow b + \eta\alpha(R_{t+1} - b) \\ 113 \quad V^\Delta(S_t) &\leftarrow V^\Delta(S_t) + \alpha(R_{t+1} - b + V^\Delta(S_{t+1}) - V^\Delta(S_t)), \\ 114 \quad \text{where } \eta \in [0, 1] \text{ produces an effective step size of } \eta\alpha \text{ for the update to } b, \text{ which usually has a slower} \\ 115 \quad \text{time-scale. This algorithm which directly averages sampled rewards is called R-learning (Schwartz,} \\ 116 \quad \text{1993). This was later improved upon by Wan et al. (2021) with the differential TD algorithm:} \\ 117 \quad \delta &= R_{t+1} - b + V^\Delta(S_{t+1}) - V^\Delta(S_t) \\ 118 \quad b &\leftarrow b + \eta\alpha\delta \\ 119 \quad V^\Delta(S_t) &\leftarrow V^\Delta(S_t) + \alpha\delta \end{aligned} \quad (1)$$

120 In addition to better empirical performance, updating  $b$  using the value update's error allows for  
 121 *off-policy* estimation of the average reward. That is,  $b$  converges to the average reward of the policy  
 122 being evaluated, allowing it to differ from that which chooses actions.

123 Recent work by Naik et al. (2024) reintroduced  $\gamma$  into Equation 1, decoupling differential TD's  
 124 reward centering mechanism from the average reward objective and demonstrating its utility on  
 125 discounted objectives. This extension was motivated by removing an often large, state-independent  
 126 offset in the value function that is evident in a value function's Laurent series decomposition:

$$127 \quad v_\pi(s) = \frac{r(\pi)}{1 - \gamma} + v_\pi^\Delta(s) + e_\pi(s, \gamma), \forall s,$$

128 where  $v_\pi(s)$  is a discounted value function,  $v_\pi^\Delta(s)$  is an undiscounted differential value function, and  
 129  $e_\pi(s, \gamma)$  is an error term that captures the difference between discounted and undiscounted values  
 130 (and vanishes as  $\gamma \rightarrow 1$ ). Subtracting  $r(\pi)$  from each reward in a discounted, infinite-horizon  
 131 return results in a subtraction of  $\frac{r(\pi)}{1 - \gamma}$  from the return, thus canceling the constant in the above  
 132 decomposition. Reward centering was shown to improve sample efficiency but remained limited to  
 133 continuing problems. In episodic problems, the shift in return from shifts in reward depends on the  
 134 remaining episode length. Because the remaining episode length varies across states and actions,  
 135 invariance of the optimal policies is not guaranteed.

136 Interestingly, differential TD is a possible explanation for the interplay between phasic and tonic  
 137 dopamine in the brain (Gershman et al., 2024). This biological plausibility further motivates devel-  
 138 oping and understanding centered TD algorithms.

### 139 3 CENTERING REWARDS IN THE PRESENCE OF TERMINATION

140 In this section, we demonstrate how to maintain invariance of the optimal policies under reward  
 141 centering. In particular, we consider a view of reward centering as potential-based reward shaping  
 142 (Ng et al., 1999). Given some function  $F(s, a, s')$  of the form:

$$143 \quad F(s, a, s') = \gamma\Phi(s') - \Phi(s),$$

144 where  $\Phi(S_T) \stackrel{\text{def}}{=} 0$ , adding  $F(s, a, s')$  to each reward maintains invariance of the optimal poli-  
 145 cies while having an effect on learning dynamics. Without assumptions on the MDP,  $r(s, a, s') +$   
 146  $F(s, a, s')$  was shown to be the only reward transformation with this property (Ng et al., 1999). For  
 147 some free variable  $b$ , if we define  $\Phi(s)$ :

$$148 \quad \Phi(s) \stackrel{\text{def}}{=} \frac{b}{1 - \gamma},$$

149 we get the following state-independent reward shaping term:

$$\begin{aligned} 150 \quad F(s, a, s') &= \gamma\frac{b}{1 - \gamma} - \frac{b}{1 - \gamma} \\ 151 \quad &= b\frac{\gamma - 1}{1 - \gamma} \\ 152 \quad &= -b. \end{aligned}$$

162 This produces a constant shift in reward. If  $b$  estimates the average reward, this shaping term in  
 163 continuing problems recovers differential TD and validates that the ordering of policies remains  
 164 unchanged. However, reward shaping makes no assumption about the problem setting—if we rec-  
 165 ognize that  $\Phi(s)$  must be zero at terminal states (Grześ, 2017), we get:

$$167 \quad F(s, a, s') = \begin{cases} \frac{-b}{1-\gamma}, & \text{if } s' \text{ is terminal} \\ -b, & \text{otherwise} \end{cases}$$

170 This leads to the following TD updates:

$$171 \quad V^\Delta(S_t) \leftarrow \begin{cases} V^\Delta(S_t) + \alpha(R_{t+1} - \frac{b}{1-\gamma} - V^\Delta(S_t)), & \text{if } s' \text{ is terminal} \\ V^\Delta(S_t) + \alpha(R_{t+1} - b + \gamma V^\Delta(S_{t+1}) - V^\Delta(S_t)), & \text{otherwise} \end{cases}$$

174 which can be equivalently expressed through the following terminal differential value definition:

$$176 \quad V^\Delta(S_t) \leftarrow V^\Delta(S_t) + \alpha(R_{t+1} - b + \gamma V^\Delta(S_{t+1}) - V^\Delta(S_t))$$

$$177 \quad V^\Delta(S_T) \stackrel{\text{def}}{=} \frac{-b}{1-\gamma}.$$

180 The intuition behind this terminal value definition lies in the equivalence between a terminal state  
 181 and an infinitely self-looping state with zero reward. The update is akin to transforming an episodic  
 182 problem into an equivalent, hypothetical continuing problem—a setting where constant shifts in  
 183 reward lead to constant shifts in return. In this view, the infinite discounted shifts in the self-  
 184 looping state are summarized with a closed-form expression. We note, however, that this episodic-  
 185 to-continuing transformation is from the *perspective of the value function*, as an agent still resets to  
 186 a starting state and does not perform updates in the terminal state.

187 Reward shaping also has an equivalence with value-function initialization (Wiewiora, 2003), sug-  
 188 gesting that it can influence exploration via means like optimistic initialization (Sun et al., 2022).  
 189 The relationship between reward shaping and value-function initialization provides insight as to why  
 190 we might expect centering to improve sample efficiency. It is akin to initializing a value function to  
 191 its mean and reducing the distance that each state- or action-value has to travel. It is not an exact  
 192 equivalence here, as  $b$  changes over time (Devlin & Kudenko, 2012). However, because we are  
 193 estimating a single scalar, it is a relatively simple learning problem.

194 Because the modification is equivalent to defining a terminal differential value, formally this is a  
 195 generalization of differential TD as the algorithm previously did not intend to encounter termination.  
 196 However, because of the division by  $1 - \gamma$  in the terminal differential value, the above modification  
 197 does not apply to undiscounted, episodic problems.

## 199 4 LEARNING EPISODIC DIFFERENTIAL VALUES

201 The previous section detailed how optimal policy invariance can be maintained when centering re-  
 202 wards in episodic problems. However, the reward shaping perspective assumes the potential function  
 203 is fixed and does not suggest if the algorithm is sound if  $b$  is continually updated. To reconcile this,  
 204 we view differential TD as learning values where the value function has an output-level bias unit  
 205 that is independent of state and action. To establish this equivalence, we define a value function to  
 206 be the sum of differential values (parameterized by  $\mathbf{w}$ ) and a *bias unit*  $b$ :

$$207 \quad V(s; \mathbf{w}, b) \stackrel{\text{def}}{=} V^\Delta(s; \mathbf{w}) + b.$$

209 With a mean-squared-value-error objective and (sample-based) gradient-descent updates (e.g., Sutton  
 210 & Barto, 2018; Mnih et al., 2015), we get:

$$212 \quad J(\mathbf{w}, b) \stackrel{\text{def}}{=} \frac{1}{2} \sum_s d(s)(v_\pi(s) - V(s; \mathbf{w}, b))^2$$

$$214 \quad \mathbf{w}_{t+1} \leftarrow \mathbf{w}_t + \alpha(v_\pi - V(S_t; \mathbf{w}_t, b_t)) \nabla_{\mathbf{w}} V^\Delta(S_t; \mathbf{w}_t)$$

$$215 \quad b_{t+1} \leftarrow b_t + \eta \alpha(v_\pi - V(S_t; \mathbf{w}_t, b_t)),$$

216 where—to emphasize the relationship with differential TD—we again specify  $\eta \in [0, 1]$  to produce  
 217 a slower time-scale, effective step-size of  $\eta\alpha$  for the bias unit update. Substituting a TD estimate of  
 218  $v_\pi$  then gives us the following error:  
 219

$$\begin{aligned} 221 \quad v_\pi - V(S_t; \mathbf{w}_t, b_t) &= R_{t+1} + \gamma V(S_{t+1}; \mathbf{w}_t, b_t) - V(S_t; \mathbf{w}_t, b_t) \\ 222 &= R_{t+1} + \gamma V^\Delta(S_{t+1}; \mathbf{w}_t) + \gamma b_t - V^\Delta(S_t; \mathbf{w}_t) - b_t \\ 223 &= R_{t+1} - (1 - \gamma)b_t + \gamma V^\Delta(S_{t+1}; \mathbf{w}_t) - V^\Delta(S_t; \mathbf{w}_t) \end{aligned}$$

226 This resembles, but does not completely match differential TD (as defined by Equation 1) in that  
 227 it has an extra  $\gamma b_t$  term. However, because the additional term only involves a state- and action-  
 228 independent scalar, we can use reparameterization to show that this update is equivalent to differenti-  
 229 al TD if we allow the bias to use a separate step size (as is the case with differential TD). Define  
 230  $\hat{b} \stackrel{\text{def}}{=} (1 - \gamma)b$  and  $\hat{\eta} \stackrel{\text{def}}{=} \eta(1 - \gamma)$ :  
 231

$$\begin{aligned} 232 \quad \mathbf{w}_{t+1} &\leftarrow \mathbf{w}_t + \alpha(R_{t+1} - \hat{b}_t + \gamma V^\Delta(S_{t+1}; \mathbf{w}_t) - V^\Delta(S_t; \mathbf{w}_t)) \nabla_{\mathbf{w}} V^\Delta(S_t; \mathbf{w}_t) \\ 233 \quad b_{t+1} &\leftarrow b_t + \eta\alpha(R_{t+1} - \hat{b}_t + \gamma V^\Delta(S_{t+1}; \mathbf{w}_t) - V^\Delta(S_t; \mathbf{w}_t)) \frac{\partial \hat{b}_t}{\partial b_t} \\ 234 \quad &\Leftrightarrow b_{t+1} \leftarrow b_t + \eta\alpha(R_{t+1} - \hat{b}_t + \gamma V^\Delta(S_{t+1}; \mathbf{w}_t) - V^\Delta(S_t; \mathbf{w}_t))(1 - \gamma) \\ 235 \quad &\Leftrightarrow b_{t+1} \leftarrow b_t + \hat{\eta}\alpha(R_{t+1} - \hat{b}_t + \gamma V^\Delta(S_{t+1}; \mathbf{w}_t) - V^\Delta(S_t; \mathbf{w}_t)) \end{aligned}$$

240 It is evident that if we set  $\eta$  and initialize  $b_0$  appropriately, and we perform updates on the same  
 241 sequence of transitions, the updates to  $\mathbf{w}$  exactly match those of differential TD. The bias-unit  
 242 step-size can also be treated as the bias unit’s activation value. This interpretation establishes an  
 243 equivalence with a specific choice of feature representation, and as a result, the analysis of linear  
 244 TD with discounting (or eventual termination) extends toward differential TD in episodic problems.  
 245 See Appendix E for a complete proof of convergence which validates this.  
 246

247 The presence of the additional  $\gamma b_t$  term prior to reparameterization results in bootstrapping off of  
 248 uncentered values (i.e.,  $V$  and not  $V^\Delta$ ). This allows us to define the sum  $V^\Delta(S_T; \mathbf{w}) + b \stackrel{\text{def}}{=} 0$   
 249 (or  $V^\Delta(S_T; \mathbf{w}) \stackrel{\text{def}}{=} -b$ ) to handle terminal states, which is what we get if we substitute  $\hat{b}$  into the  
 250 terminal differential value definition from Section 3. This highlights that the additional  $\gamma b_t$  is what  
 251 follows from a potential function  $\Phi(s) = b$ . While the two forms are equivalent through the separate  
 252 step size, it is notably a form which is applicable in episodic problems with  $\gamma = 1$ . As an example,  
 253 Algorithm 1 details how we can extend differential Q-learning to handle episodic problems. It  
 254 provides two forms of the update which, when  $\gamma = 1$ , must be selected based on whether the  
 255 problem is known to be continuing or episodic. Either form is applicable when  $\gamma < 1$ , and as shown  
 256 above, are formally equivalent under corresponding parameter settings.  
 257

258 The connection with a choice of feature representation highlights that  $b$  and  $V^\Delta(s; \mathbf{w})$  are jointly  
 259 optimized under a common objective. This may contrast intuition from the average reward setting  
 260 where it is often presented as two interacting processes: an average reward estimate which depends  
 261 on the policy derived from differential value estimates, and differential value estimates which depend  
 262 on the average reward estimate. This view also presents an interpretation of  $\eta$  as balancing credit  
 263 assignment, which—on a problem dependent basis—may not need to be on a slower time scale.  
 264

265 The bias unit perspective further suggests what  $b$  converges to in episodic problems. It is less infor-  
 266 mative to consider average reward because any policy which eventually terminates has zero average  
 267 reward due to the equivalence between terminal states and infinite self-loops with zero reward. Be-  
 268 cause updates are not performed to the values of terminal states, the differential values are centered  
 269 over non-terminal states, making  $b$  approach the expected state-value over the (non-terminal) visi-  
 270 tation distribution, subdivided over the expected remaining episode length:  $\mathbb{E}_{s \sim d_\pi}[V(s) \frac{1 - \gamma}{1 - \gamma T(s)}]$ ,  
 271 where  $d_\pi$  represents normalized expected state visitation counts under policy  $\pi$  and  $T(s)$  is the  
 272 expected remaining episode length from state  $s$  (See Appendix C).  
 273

270 **Algorithm 1** (Generalized) Differential Q-learning

---

```

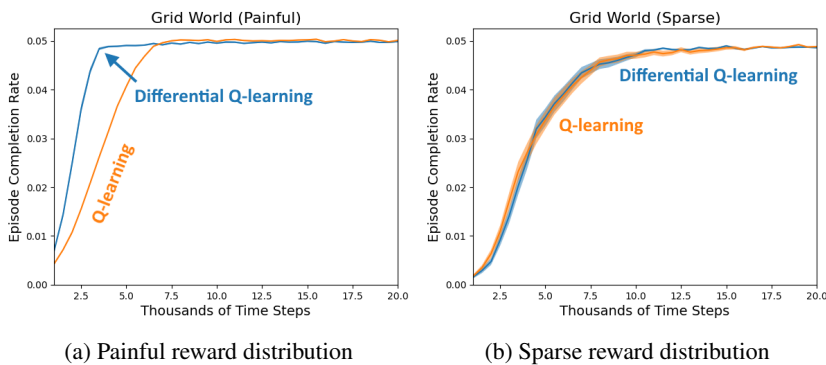
271     Initialize weights  $\mathbf{w} \in \mathbb{R}^d$  arbitrarily
272     Initialize  $b \in \mathbb{R}$  arbitrarily
273     for each episode do
274          $s \sim p(s_0)$ 
275         for each step of episode do
276              $a \sim \pi(\cdot|s)$ 
277              $s', r \sim p(s', r|s, a)$ 
278             if  $s'$  is terminal then
279                  $\delta \leftarrow r - \frac{b}{1-\gamma} - Q^\Delta(s, a; \mathbf{w})$   $\triangleright \gamma < 1$ 
280                  $\delta \leftarrow r - b - Q^\Delta(s, a; \mathbf{w})$   $\triangleright \gamma < 1$  or  $\gamma = 1$ , episodic
281             else
282                  $\delta \leftarrow r - b + \gamma \max_{a'} Q^\Delta(s', a'; \mathbf{w}) - Q^\Delta(s, a; \mathbf{w})$   $\triangleright \gamma < 1$  or  $\gamma = 1$ , continuing
283                  $\delta \leftarrow r - (1 - \gamma)b + \gamma \max_{a'} Q^\Delta(s', a'; \mathbf{w}) - Q^\Delta(s, a; \mathbf{w})$   $\triangleright \gamma < 1$  or  $\gamma = 1$ , episodic
284             end if
285              $\mathbf{w} \leftarrow \alpha \delta \nabla_{\mathbf{w}} Q^\Delta(s, a; \mathbf{w})$ 
286              $b \leftarrow \eta \alpha \delta$ 
287              $s \leftarrow s'$ 
288         end for
289     end for
290

```

---

291 **5 EMPIRICAL EVALUATION**

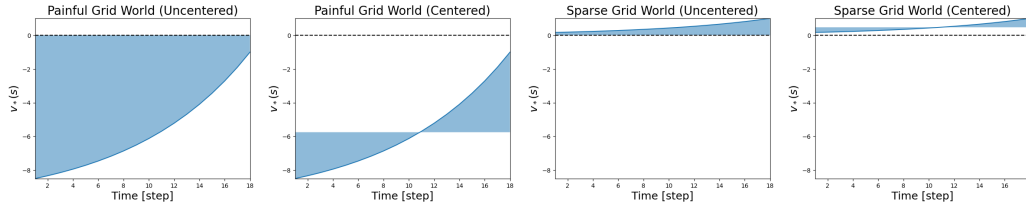
292 To see whether the benefits of centering in continuing problems (Naik et al., 2024) can be achieved  
293 in episodic problems, we consider differential Q-learning (Watkins, 1989) with our novel terminal  
294 differential value definition (Algorithm 1) and compare it with vanilla, uncentered Q-learning in a  
295  $10 \times 10$  episodic grid world where the top-left is the start state and the bottom-right is terminal. The  
296 grid world uses 4-directional movement where attempting to leave the grid keeps the agent in place.  
297 To gain insight into when centering is useful, we consider two reward distributions:  $-1$  per step  
298 (the *painful* grid world) and  $0$  per step with  $1$  upon termination (the *sparse* grid world). Based on  
299 the intuition around centering reducing the total distance that outputs need to travel, our hypothesis  
300 is that centering will provide substantially more benefit in the painful grid world, since the values  
301 deviate more across states. We fixed  $\gamma = 0.9$ , tuned  $\alpha$  for Q-learning, and we tuned  $\alpha$  and  $\eta$  for  
302 differential Q-learning. An  $\epsilon$ -greedy policy was used for both algorithms with  $\epsilon = 0.1$ . Full details  
303 of the parameter sweeps can be found in Appendix A.



315 Figure 1: Performance of Q-learning when used with reward- and value-centering compared against  
316 a standard uncentered baseline. The results are averaged over 100 independent runs where the  
317 shaded areas (occasionally less than a line width) represent the standard error.

318  
319 Figure 1 shows the average rate of completed episodes per environment step of each algorithm's  
320 best parameter setting in terms of total episodes completed, for each reward distribution. With the  
321 painful reward distribution, differential Q-learning improves significantly over the uncentered base-  
322 line. However, in the sparse reward variant, both algorithms performed similarly. Recognizing  
323 that both algorithms performed worse with sparse rewards, it is possible that learning was bottle-  
324 necked by having a comparatively difficult exploration problem. Nevertheless, this validates that

324 there is benefit to centering in episodic problems. The results further suggest that the benefit can  
 325 be expected when there is greater value-deviation across states (typical of dense reward settings),  
 326 consistent with the intuition of centering reducing the distance that outputs need to travel. The value  
 327 deviation along the optimal path is visualized in Figure 2.



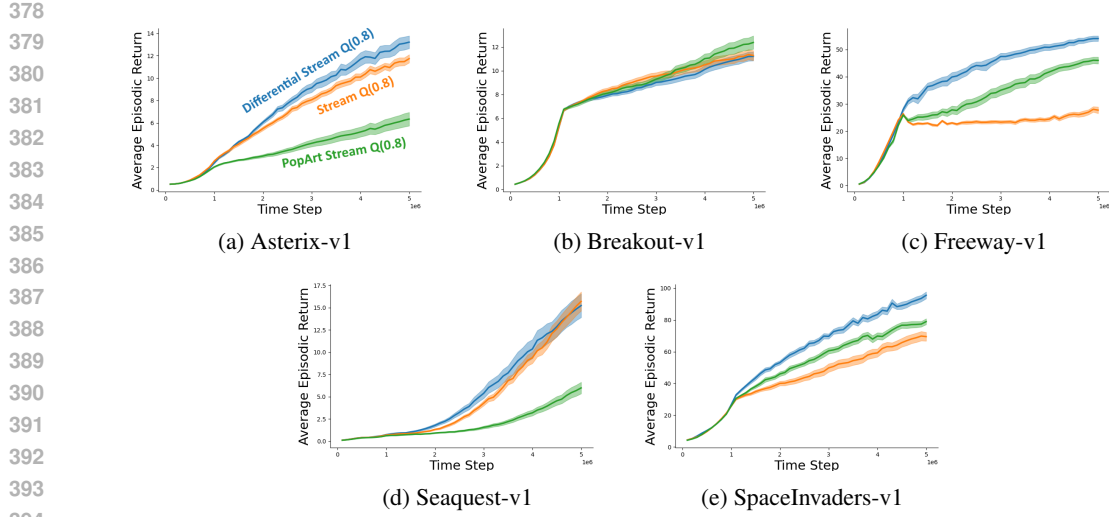
331  
 332  
 333  
 334  
 335  
 336  
 337  
 338 Figure 2: Uncentered and centered output distances (shaded area) along the optimal path in the  
 339 Painful and Sparse Grid World environments. Because the Sparse Grid World’s values are relatively  
 340 small and concentrated around zero, we might expect less benefit from centering.

341  
 342  
 343 To further validate that centering can be done in episodic problems without changing the underlying  
 344 problem and to demonstrate that there is benefit in doing so, we examine more challenging environ-  
 345 ments that require non-linear function approximation. Specifically, we extend two streaming deep  
 346 reinforcement learning algorithms: Stream Q( $\lambda$ ) and Stream AC( $\lambda$ ) (Elsayed et al., 2024) to their  
 347 differential counterparts. We additionally compare against PopArt (van Hasselt et al., 2016)—an al-  
 348 gorithm which similarly employs output centering but with explicit attention on precisely preserving  
 349 the unnormalized outputs. When using PopArt normalization with Stream Q( $\lambda$ ) or Stream AC( $\lambda$ ),  
 350 we omit reward scaling as PopArt performs its own output scaling. We provide further experimental  
 351 details and hyperparameters used in Appendix B.

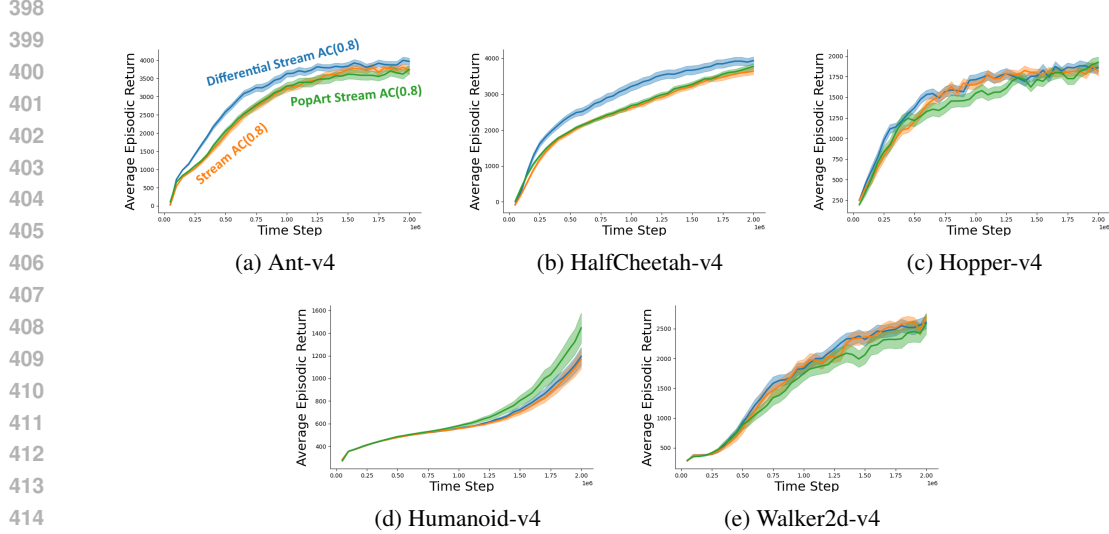
352 Figure 3 shows the performance of Stream Q( $\lambda$ ), differential Stream Q( $\lambda$ ), and PopArt Stream Q( $\lambda$ )  
 353 on Asterix, Breakout, Freeway, Seaquest, and SpaceInvaders from the MinAtar suite (Young & Tian,  
 354 2019). We tune  $\eta$  and present results under the best-performing parameters from our search. We ob-  
 355 serve that differential Stream Q( $\lambda$ ) improves over its uncentered base algorithm in all environments  
 356 except for Breakout, where they perform similarly. On the other hand, PopArt normalization with  
 357 Stream Q( $\lambda$ ) was less consistent across the environments. It is unclear why this is the case because  
 358 PopArt had not previously been demonstrated in a streaming deep reinforcement learning setup, and  
 359 had not been used in these environments. It may be a nuance around explicitly normalizing the  
 360 outputs with specific statistics and trying to precisely preserve outputs as these statistics may shift,  
 361 in contrast with differential TD which jointly optimizes the shift under the same objective.

362 Next, we compare our centering approach in continuous-action control. In Figure 4, we show the  
 363 performance of Stream AC( $\lambda$ ), differential Stream AC( $\lambda$ ), and PopArt Stream AC( $\lambda$ ) in the MuJoCo  
 364 suite (Todorov et al., 2012). It can be observed in Figure 4 that differential Stream AC( $\lambda$ ) showed  
 365 considerable improvement in the Ant-v4 and HalfCheetah-v4 environments, while not performing  
 366 worse than its uncentered counterpart in the remaining ones. Notably, these two environments saw  
 367 the largest return magnitudes over the duration of a run, which may be related to large value devia-  
 368 tions across states. PopArt did not demonstrate statistically significant improvement in this suite.

369 Lastly, to explicitly validate the insight from the grid world experiments on when differential TD  
 370 helps, we modified the Deepmind Control Suite’s Reacher environment Tassa et al. (2018). Specifi-  
 371 cally, we created a *Painful* Reacher environment that receives a reward of  $-1$  per step to mirror the  
 372 grid world set up that showed substantial benefit. To lengthen episode duration and consequently  
 373 increase value magnitudes and deviation, we additionally evaluate in a harder variant of the task  
 374 that shrinks the goal location. With results presented in Figure 5, we see significant improvement  
 375 in using differential Stream AC( $\lambda$ ) over the uncentered base algorithm. Taking all of the evaluation  
 376 together, we have established that reward centering can be done in episodic problems and that it can  
 377 improve sample efficiency over uncentered algorithms. We further observed that the differential ex-  
 378 tension, when tuned, never performed worse than its base algorithm. This is to be expected because  
 379 the  $\eta = 0$  extreme results in a standard, uncentered TD update.



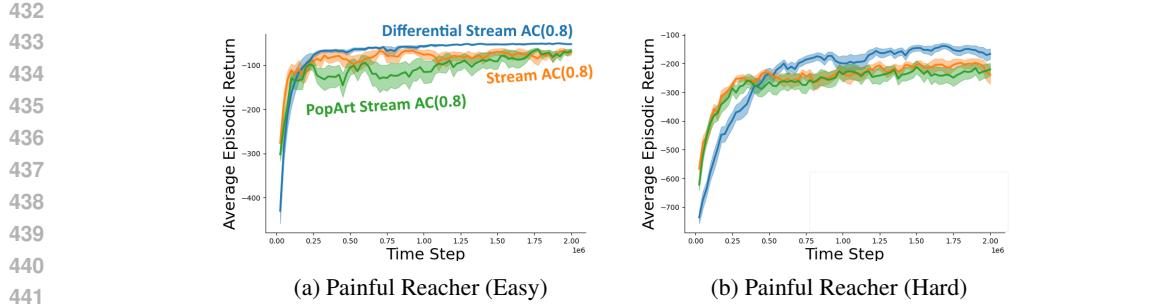
395 Figure 3: Performance of differential Stream Q(0.8) compared against a standard uncentered base-  
 396 line and a PopArt-normalized baseline in the MinAtar suite. The results are averaged over 30 inde-  
 397 pendent runs where the shaded areas represent the standard error.



416 Figure 4: Performance of differential Stream AC(0.8) compared against a standard uncentered base-  
 417 line and a PopArt-normalized baseline in the MuJoCo suite. The results are averaged over 30 inde-  
 418 pendent runs where the shaded areas represent the standard error.

## 420 6 CONCLUSIONS, DISCUSSION, AND FUTURE WORK

423 In this work, we explored the reward centering mechanism of differential TD algorithms, which was  
 424 previously limited to infinite-horizon reinforcement learning problems. By viewing reward centering  
 425 from the lens of potential-based reward shaping, we propose a differential terminal value definition  
 426 which—when used—maintains the ordering of policies and strictly generalizes differential TD to be  
 427 applicable in episodic problems. We further show equivalence between the generalized differential  
 428 TD update and an output-level, state- and action-independent bias unit. This establishes that the  
 429 algorithm shares the theoretical guarantees previously shown for linear TD, and provides insight  
 430 into how the centering term can be interpreted in an episodic problem. In a tabular environment,  
 431 we demonstrated that centering can improve sample efficiency in episodic problems and provided  
 432 arguments for when such benefits might be expected. In a streaming deep reinforcement learning  
 433 setup, we further showed that these algorithms can scale to difficult problems with non-linear func-



442  
443  
444  
445  
446  
447  
448  
449  
450  
451  
452  
453  
454  
455  
456  
457  
458  
459  
460  
461  
462  
463  
464  
465  
466  
467  
468  
469  
470  
471  
472  
473  
474  
475  
476  
477  
478  
479  
480  
481  
482  
483  
484  
485

Figure 5: Performance of differential Stream AC(0.8) compared against a standard uncentered baseline and a PopArt-normalized baseline in the Painful Reacher environment. The results are averaged over 30 independent runs where the shaded areas represent the standard error.

tion approximation. Altogether, we have shown that reward centering can be applied in the presence of termination without altering the underlying task, and that doing so is beneficial.

There are many avenues for future work. Our evaluation focused on the streaming reinforcement learning setting, as that is where normalization was recently shown to have substantial benefit. However—as emphasized by Naik et al. (2024)—reward centering is a relatively general idea that can be easily dropped into any existing algorithm. Broadening its applicability toward episodic environments, the scope of possible comparisons between algorithms is larger now and there is merit in investigating differential TD’s utility toward other types of episodic reinforcement learning algorithms (e.g., ones which store and process explicit episode trajectories). While the additional step-size parameter  $\eta$  was already present in the original differential TD algorithms, the additional overhead in tuning this parameter remains a limitation. Given that centering involves learning a single scalar—a seemingly simple learning problem—it would be promising to explore whether  $\eta$  can be efficiently meta-learned (e.g., Sutton, 1992; Mahmood et al., 2012; Sharifnassab et al., 2024).

## REFERENCES

J. L. Ba, J. R. Kiros, and G. E. Hinton. Layer normalization. *CoRR*, abs/1607.06450, 2016.

Vivek S Borkar. *Stochastic approximation: a dynamical systems viewpoint*, volume 100. Springer, 2008.

S. Devlin and D. Kudenko. Dynamic potential-based reward shaping. In *Proceedings of the International Conference on Autonomous Agents and Multiagent Systems*, 2012.

M. Elsayed, G. Vasan, and A. R. Mahmood. Streaming deep reinforcement learning finally works. *CoRR*, abs/2410.14606, 2024.

S. J. Gershman, J. A. Assad, S. R. Datta, S. W. Linderman, B. L. Sabatini, N. Uchida, and L. Wilbrecht. Explaining dopamine through prediction errors and beyond. *Nature Neuroscience*, 27, 2024.

M. Grześ. Reward shaping in episodic reinforcement learning. In *Proceedings of the International Conference on Autonomous Agents and Multiagent Systems*, 2017.

H. Lee, Y. Lee, T. Seno, D. Kim, P. Stone, and J. Choo. Hyperspherical normalization for scalable deep reinforcement learning. *CoRR*, abs/2502.15280, 2025.

C. Lyle, Z. Zheng, E. Nikishin, B. A. Pires, R. Pascanu, and W. Dabney. Understanding plasticity in neural networks. In *Proceedings of the International Conference on Machine Learning*, 2023.

C. Lyle, Z. Zheng, K. Khetarpal, J. Martens, H. van Hasselt, R. Pascanu, and W. Dabney. Normalization and effective learning rates in reinforcement learning. *CoRR*, abs/2407.01800, 2024.

S. Mahadevan. Average reward reinforcement learning: foundations, algorithms, and empirical results. *Machine Learning*, 1996.

486 A. R. Mahmood, R. S. Sutton, T. Degris, and P. M. Pilarski. Tuning-free step-size adaptation. In  
 487 *Proceedings of the IEEE International Conference on Acoustics, Speech and Signal Processing*,  
 488 2012.

489 V. Mnih, K. Kavukcuoglu, D. Silver, A. A. Rusu, J. Veness, M. G. Bellemare, A. Graves, M. Ried-  
 490 miller, A. K. Fidjeland, G. Ostrovski, S. Petersen, C. Beattie, A. Sadik, I. Antonoglou, H. King,  
 491 D. Kumaran, D. Wierstra, S. Legg, and D. Hassabis. Human-level control through deep reinforce-  
 492 ment learning. *Nature*, 518, 2015.

493 A. Naik. *Reinforcement learning for continuing problems using average reward*. PhD thesis, Uni-  
 494 versity of Alberta, 2024.

495 A. Naik, Y. Wan, M. Tomar, and R. S. Sutton. Reward centering. *Reinforcement Learning Journal*,  
 496 2024.

497 A. Y. Ng, D. Harada, and S. Russell. Policy invariance under reward transformations: theory and  
 498 application to reward shaping. In *Proceedings of the International Conference on Machine Learn-  
 499 ing*, 1999.

500 D. Palenicek, F. Vogt, and J. Peters. Scaling off-policy reinforcement learning with batch and weight  
 501 normalization. *CoRR*, abs/2502.07523, 2025.

502 A. Schwartz. A reinforcement learning method for maximizing undiscounted rewards. In *Proceed-  
 503 ings of the International Conference on Machine Learning*, 1993.

504 A. Sharifnassab, S. Salehkaleybar, and R. S. Sutton. MetaOptimize: a framework for optimizing  
 505 step sizes and other meta-parameters. *CoRR*, abs/2402.02342, 2024.

506 H. Sun, L. Han, R. Yang, X. Ma, J. Guo, and B. Zhou. Exploit reward shifting in value-based  
 507 deep-RL: optimistic curiosity-based exploration and conservative exploitation via linear reward  
 508 shaping. In *Advances in Neural Information Processing Systems*, 2022.

509 R. S. Sutton. NADALINE: a normalized adaptive linear element that learns efficiently, 1988a.  
 510 Technical report.

511 R. S. Sutton. Learning to predict by the methods of temporal differences. *Machine Learning*, 1988b.

512 R. S. Sutton. Adapting bias by gradient descent: an incremental version of Delta-Bar-Delta. *Pro-  
 513 ceedings of the AAAI Conference on Artificial Intelligence*, 1992.

514 R. S. Sutton. TD models: modeling the world at a mixture of time scales. In *Proceedings of the  
 515 International Conference on Machine Learning*, 1995.

516 R. S. Sutton and A. G. Barto. *Reinforcement learning: an introduction*. MIT Press, 2nd edition,  
 517 2018.

518 R. S. Sutton, J. Modayil, M. Delp, T. Degris, and D. Precup. Horde: a scalable real-time architec-  
 519 ture for learning knowledge from unsupervised sensorimotor interaction. In *Proceedings of the  
 520 International Conference on Autonomous Agents and Multiagent Systems*, 2011.

521 Y. Tassa, Y. Doron, A. Muldal, T. Erez, Y. Li, D. Casas, D. Budden, A. Abdolmaleki, J. Merel,  
 522 A. Lefrancq, T. Lillicrap, and M. Riedmiller. DeepMind control suite. *CoRR*, abs/1801.00690,  
 523 2018.

524 E. Todorov, T. Erez, and Y. Tassa. MuJoCo: a physics engine for model-based control. In *Proceed-  
 525 ings of the IEEE/RSJ International Conference on Intelligent Robots and Systems*, 2012.

526 M. Towers, A. Kwiatkowski, J. Terry, J. U. Balis, G. De Cola, T. Deleu, M. Goulão, A. Kallinteris,  
 527 M. Krimmel, A. KG, R. Perez-Vicente, A. Pierré, S. Schulhoff, J. J. Tai, H. Tan, and O. G.  
 528 Younis. Gymnasium: a standard interface for reinforcement learning environments. *CoRR*,  
 529 abs/2407.17032, 2024.

530 JN Tsitsiklis and B Van Roy. An analysis of temporal-difference learning with function approxima-  
 531 tion. *IEEE Transactions on Automatic Control*, 42(5):674–690, 1997.

540 H. van Hasselt, A. Guez, M. Hessel, V. Mnih, and D. Silver. Learning values across many orders of  
541 magnitude. In *Advances in Neural Information Processing Systems*, 2016.

542

543 G. Vassan, M. Elsayed, S. A. Azimi, J. He, F. Shahriar, C. Bellinger, M. White, and A. R. Mah-  
544 mood. Deep policy gradient methods without batch updates, target networks, or replay buffers.  
545 In *Advances in Neural Information Processing Systems*, 2024.

546

547 Y. Wan, A. Naik, and R. S. Sutton. Learning and planning in average-reward Markov decision  
548 processes. In *Proceedings of the International Conference on Machine Learning*, 2021.

549

550 C. J. C. H. Watkins. *Learning from delayed rewards*. PhD thesis, King's College, 1989.

551

552 M. White. Unifying task specification in reinforcement learning. *CoRR*, abs/1609.01995, 2016.

553

554 E. Wiewiora. Potential-based shaping and Q-value initialization are equivalent, 2003. Technical  
555 report.

556

557

558

559

560

561

562

563

564

565

566

567

568

569

570

571

572

573

574

575

576

577

578

579

580

581

582

583

584

585

586

587

588

589

590

591

592

593

594 A EXPERIMENTAL DETAILS OF GRID WORLD EXPERIMENTS  
595596  
597 We swept over  $\alpha \in \{0.1, 0.2, 0.3, 0.4, 0.5, 0.6, 0.7, 0.8, 0.9, 1.0\}$  for both algorithms and  $\eta \in$   
598  $\{10^{-4}, 10^{-3.5}, 10^{-3}, 10^{-2.5}, 10^{-2}, 10^{-1.5}, 10^{-1}, 10^{-0.5}, 10^0\}$  for differential Q-learning. In the  
599 painful grid world,  $\alpha = 1.0$  was best for both algorithms, with  $\eta = 10^{-3}$  performing best for dif-  
600 fferential Q-learning. In the sparse grid world,  $\alpha = 0.9$  was best for both algorithms, with  $\eta = 10^{-4}$   
601 performing best for differential Q-learning.  
602603 B EXPERIMENTAL DETAILS OF STREAMING DEEP RL EXPERIMENTS  
604605  
606 We swept over bias step-sizes  $\eta \in \{10^{-2}, 10^{-1}, 10^0, 10^1, 10^2, 10^3\}$ , and we show performance with  
607 the best-performing value. For Stream AC, we used step-size  $\alpha = 1$ ,  $\kappa_\pi = 3$ ,  $\kappa_v = 2$ ,  $\lambda = 0.8$ ,  
608 discount factor  $\gamma = 0.99$ , and entropy coefficient  $\tau = 0.01$ . For Stream Q, we used step-size  $\alpha = 1$ ,  
609  $\kappa_v = 2$ ,  $\lambda = 0.8$ , discount factor  $\gamma = 0.99$ . We used the same neural network architectures used  
610 with Stream AC and Stream Q reported by [Elsayed et al. \(2024\)](#). Lastly, we used an  $\epsilon$ -greedy policy  
611 where  $\epsilon$  linearly decayed from 1 to 0.01 within 20% of the total time steps of a run.  
612613 C b'S INTERPRETATION IN AN EPISODIC PROBLEM  
614615  
616 Prior average reward definitions lead to zero average reward in episodic problems (due to the equiv-  
617 alence between terminal states and an infinite loop of zero reward), that it is more informative to  
618 consider the bias-unit perspective in understanding what  $b$  tends toward. Under a squared loss, the  
619 minimizing bias is the expectation of the targets under the behavior distribution. However, the bias  
620 is applied on a *reward level*, suggesting that  $b$  is related to the expected state-value, but subdivided  
621 over the time remaining in an episode and discounted appropriately:  
622

623 
$$\mathbb{E}_{s \sim d_\pi} \left[ \sum_{k=0}^{T-t-1} \gamma^k (R_{t+k+1} - b) \middle| s = S_t \right] = 0$$
  
624 
$$\mathbb{E}_{s \sim d_\pi} \left[ \sum_{k=0}^{T-t-1} \gamma^k b \middle| s = S_t \right] = \mathbb{E}_{s \sim d_\pi} \left[ \sum_{k=0}^{T-t-1} \gamma^k R_{t+k+1} \middle| s = S_t \right]$$
  
625 
$$\mathbb{E}_{s \sim d_\pi} \left[ b \frac{1 - \gamma^{T-t}}{1 - \gamma} \middle| s = S_t \right] = \mathbb{E}_{s \sim d_\pi} [v_\pi(s)]$$
  
626 
$$\mathbb{E}_{s \sim d_\pi} \left[ b \frac{1 - \gamma^{T(s)}}{1 - \gamma} \right] = \mathbb{E}_{s \sim d_\pi} [v_\pi(s)]$$
  
627 
$$b = \mathbb{E}_{s \sim d_\pi} \left[ v_\pi(s) \frac{1 - \gamma}{1 - \gamma^{T(s)}} \right]$$
  
628

629 where  $d_\pi$  represents normalized expected state visitation counts over non-terminal states under pol-  
630 icy  $\pi$  and  $T(s)$  is the expected remaining episode length from state  $s$ .  
631642 D EPISODIC PROBLEMS AS STATE-DEPENDENT DISCOUNTING  
643644  
645 It has been previously acknowledged that episodic problems can be implemented as infinite-horizon  
646 problems with a state-dependent discount function ([Sutton, 1995](#); [Sutton et al., 2011](#); [White, 2016](#)).  
647 For example, we can have  $\gamma(s') = 0$  if  $s'$  is terminal, and have it equal to the problem's discount  
648 otherwise. The terminal state would then transition back to a start state.  
649

648 Consider an infinite-horizon return with potential-based reward shaping and state-dependent dis-  
 649 counting. We define  $\gamma_t \stackrel{\text{def}}{=} \gamma(S_t)$  for notational convenience:  
 650

$$\begin{aligned}
 651 \quad G_t^\Phi &\stackrel{\text{def}}{=} \sum_{k=t}^{\infty} \left( \prod_{i=t+1}^k \gamma_i \right) (R_{k+1} + F(S_k, A_k, S_{k+1})) \\
 652 \quad &= \sum_{k=t}^{\infty} \left( \prod_{i=t+1}^k \gamma_i \right) (R_{k+1} + \gamma_{k+1} \Phi(S_{k+1}) - \Phi(S_k)) \\
 653 \quad &= \sum_{k=t}^{\infty} \left( \prod_{i=t+1}^k \gamma_i \right) R_{k+1} + \sum_{k=t}^{\infty} \left( \prod_{i=t+1}^k \gamma_i \right) \gamma_{k+1} \Phi(S_{k+1}) - \sum_{k=t}^{\infty} \left( \prod_{i=t+1}^k \gamma_i \right) \Phi(S_k) \\
 654 \quad &= \sum_{k=t}^{\infty} \left( \prod_{i=t+1}^k \gamma_i \right) R_{k+1} + \sum_{k=t+1}^{\infty} \left( \prod_{i=t+1}^k \gamma_i \right) \Phi(S_k) - \sum_{k=t+1}^{\infty} \left( \prod_{i=t+1}^k \gamma_i \right) \Phi(S_k) - \Phi(S_t) \\
 655 \quad &= \sum_{k=t}^{\infty} \left( \prod_{i=t+1}^k \gamma_i \right) R_{k+1} - \Phi(S_t)
 \end{aligned}$$

666 Due to the Markov property, the subtraction of  $\Phi(S_t)$  will not impact the ordering of policies.  
 667 This also highlights that the learned values are relative to the potential function (i.e., it is akin to  
 668 initializing the value function to  $\Phi(s)$ ). Let us now consider the following potential function:  
 669

$$\Phi(s) \stackrel{\text{def}}{=} \frac{b}{1 - \gamma(s)}$$

670 If we implement an episodic problem by defining  $\gamma(S_T) \stackrel{\text{def}}{=} 0$  and modifying the transition dynamics  
 671 such that terminal states transition to a starting state sampled from a starting state distribution  
 672 (independent of action), there are three scenarios:  
 673

$$F(s, a, s') = \begin{cases} -\frac{b}{1-\gamma(s)}, & \text{if } \gamma(s') = 0 \\ \gamma(s') \frac{b}{1-\gamma(s')} - b, & \text{if } \gamma(s) = 0 \\ \gamma(s') \frac{b}{1-\gamma(s')} - \frac{b}{1-\gamma(s)}, & \text{otherwise} \end{cases}$$

674 If we assume that all non-zero discounts are constant (i.e.,  $\gamma_t = \gamma$ ), this simplifies to:  
 675

$$F(s, a, s') = \begin{cases} -\frac{b}{1-\gamma}, & \text{if } \gamma(s') = 0 \\ \gamma \frac{b}{1-\gamma} - b, & \text{if } \gamma(s) = 0 \\ -b, & \text{otherwise} \end{cases}$$

676 This resembles the result in Section 3, except we have an additional  $\gamma \frac{b}{1-\gamma}$  term in the case where  
 677  $\gamma(s) = 0$ . This term is set up to cancel with a portion of the previous time step's  $-\frac{b}{1-\gamma}$  term, leaving  
 678  $-b$  behind. However, this case corresponds with transitioning *from* a terminal state. Because we do  
 679 not typically learn values for terminal states, this target typically will not be used. The remaining  
 680 scenarios are consistent with what we get from the explicit episodic return.  
 681

## 694 E CONVERGENCE OF EPISODIC DIFFERENTIAL TD

695 In this section, we analyze the asymptotic convergence of the Differential TD algorithm with dis-  
 696 counting. We focus on linear function approximation,  $V(s) = \phi(s)^\top w$ , which subsumes the tabular  
 697 case.  
 698

699 We adopt the Ordinary Differential Equation (ODE) method for stochastic approximation (Borkar,  
 700 2008). We first define the update rules and the expanded parameter space. Crucially, we utilize an  
 701 *unrolled MDP* formulation to unify the analysis of continuing and episodic tasks.  
 702

702 E.1 UPDATE RULES AND EXPANDED FEATURES  
703

704 The differential TD algorithm maintains a parameter vector  $\mathbf{w}$  and a separate scalar bias estimate  $b$   
705 (related to the average reward or reward offset). The update for a transition  $(S_t, A_t, R_{t+1}, S_{t+1})$  is  
706 given by:

707  $\mathbf{w}_{t+1} = \mathbf{w}_t + \alpha_t \delta_t \phi(S_t), \quad (2)$   
708

709  $b_{t+1} = b_t + \eta \alpha_t \delta_t. \quad (3)$

710 Here,  $\alpha_t$  is the learning rate and  $\eta > 0$  is a scalar multiplier for the bias learning rate. Based on  
711 Section 4, The TD error  $\delta_t$  is defined as:

- 712 • **Continuing:**  $\delta_t = R_{t+1} - (1 - \gamma)b_t + \gamma\phi(S_{t+1})^\top \mathbf{w}_t - \phi(S_t)^\top \mathbf{w}_t.$
- 713 • **Episodic (Non-terminal):** Same as above.
- 714 • **Episodic (Terminal):**  $\delta_t = R_{t+1} - b_t - \phi(S_t)^\top \mathbf{w}_t.$

715 To analyze this coupled system, we augment the feature vector to include a bias unit, forming the  
716 expanded feature vector  $\tilde{\phi}(s) = [\mathbb{I}(s), \phi(s)^\top]^\top \in \mathbb{R}^{d+1}$ . The corresponding parameter vector is  
717  $\tilde{\mathbf{w}} = [b, \mathbf{w}^\top]^\top$ . Here,  $\mathbb{I}(s)$  acts as the bias feature: it is 1 for all states in the continuing setting, and  
718  $[\mathbf{e}]_s$  (indicator of non-terminal status) in the episodic setting.

719 The updates can be rewritten in a unified form:

720  $\tilde{\mathbf{w}}_{t+1} = \tilde{\mathbf{w}}_t + \alpha_t \delta_t \mathbf{K} \tilde{\phi}(S_t), \quad (4)$

721 where  $\mathbf{K} = \text{diag}(\eta, 1, \dots, 1)$  handles the separate learning rate scaling, and the TD error simplifies  
722 to:

723  $\delta_t = R_{t+1} + \gamma \tilde{\phi}(S_{t+1})^\top \tilde{\mathbf{w}}_t - \tilde{\phi}(S_t)^\top \tilde{\mathbf{w}}_t. \quad (5)$

724 In the episodic case, we define  $\tilde{\phi}(S_{\text{term}}) \equiv \mathbf{0}$ .

## 725 E.2 ASSUMPTIONS AND UNROLLED MDP

726 To provide a single convergence proof, we model the episodic setting as a continuing process and  
727 formalize our assumptions.

728 **Definition 1** (Unrolled MDP). *For an episodic task, the Unrolled MDP is a continuing Markov chain  
729 constructed by treating the sequence of episodes as a single stream. Upon reaching a terminal state  
730  $s_T$ , the process transitions at the next time step to a start state  $s_0$  sampled from the initial distribution  
731  $d_0$ .*

732 We define the unified transition matrix  $\mathbf{P}_\pi$  and stationary distribution matrix  $\mathbf{D}_\pi$  (diagonal matrix  
733 of the stationary distribution  $d_\pi$ ) based on this unrolled view.

734 **Assumption 1** (Ergodicity). *The Markov chain induced by the policy  $\pi$  (or the Unrolled MDP in  
735 the episodic case) is ergodic (irreducible and aperiodic), admitting a unique stationary distribution  
736  $d_\pi$ .*

737 **Assumption 2** (Linearly Independent Features). *The expanded feature matrix  $\tilde{\Phi}$  has full column  
738 rank.*

739

- 740 • *Continuing:*  $\tilde{\Phi} = [\mathbf{1}, \Phi]$ .
- 741 • *Episodic:*  $\tilde{\Phi} = [\mathbf{e}, \Phi]$ , where  $\mathbf{e}$  is zero for terminal states.

742 Furthermore, for all  $s$ ,  $\|\phi(s)\| < \infty$ .

743 **Assumption 3** (Step Sizes and Noise). *The step sizes  $\alpha_t$  satisfy the standard Robbins-Monro con-  
744 ditions:  $\sum_{t=0}^{\infty} \alpha_t = \infty$  and  $\sum_{t=0}^{\infty} \alpha_t^2 < \infty$ . The reward function has bounded variance.*

## 745 E.3 CONVERGENCE ANALYSIS

746 The behavior of the stochastic update in Equation 4 is governed by the mean field ODE:

747  $\dot{\tilde{\mathbf{w}}} = \mathbf{K}(\tilde{\mathbf{A}}\tilde{\mathbf{w}} + \tilde{\mathbf{b}}), \quad (6)$

756 where  $\tilde{\mathbf{b}} = \mathbb{E}[R_{t+1}\tilde{\phi}(S_t)]$  and  $\tilde{\mathbf{A}}$  is the expected update direction matrix:  
 757

$$758 \quad \tilde{\mathbf{A}} = \tilde{\Phi}^\top \mathbf{D}_\pi (\gamma \mathbf{P}_\pi - \mathbf{I}) \tilde{\Phi}. \quad (7)$$

759 **Theorem 1.** Let  $\gamma < 1$  and  $\eta > 0$ . Under Assumptions 1, 2, and 3, the parameter  $\tilde{\mathbf{w}}_t$  converges  
 760 with probability 1 to the unique fixed point  $\tilde{\mathbf{w}}^* = -\tilde{\mathbf{A}}^{-1}\tilde{\mathbf{b}}$ .  
 761

762 *Proof.* The proof proceeds in two steps. First, we show that  $\tilde{\mathbf{A}}$  is negative definite. Second, we  
 763 show that the preconditioning by  $\mathbf{K}$  preserves stability.  
 764

765 **Step 1: Negative Definiteness of  $\tilde{\mathbf{A}}$ .** Consider the quadratic form for an arbitrary vector  $\mathbf{x} \neq \mathbf{0}$ .  
 766 Let  $\mathbf{y} = \tilde{\Phi}\mathbf{x}$ . By Assumption 2 (full rank),  $\mathbf{y} \neq \mathbf{0}$ .  
 767

$$768 \quad \mathbf{x}^\top \tilde{\mathbf{A}} \mathbf{x} = \mathbf{y}^\top \mathbf{D}_\pi (\gamma \mathbf{P}_\pi - \mathbf{I}) \mathbf{y} = \gamma \langle \mathbf{y}, \mathbf{P}_\pi \mathbf{y} \rangle_{\mathbf{D}_\pi} - \|\mathbf{y}\|_{\mathbf{D}_\pi}^2. \quad (8)$$

770 The transition operator is a non-expansion in the  $\mathbf{D}_\pi$ -weighted norm (Tsitsiklis & Van Roy, 1997).  
 771 Applying the Cauchy-Schwarz inequality:

$$772 \quad \langle \mathbf{y}, \mathbf{P}_\pi \mathbf{y} \rangle_{\mathbf{D}_\pi} \leq \|\mathbf{y}\|_{\mathbf{D}_\pi} \|\mathbf{P}_\pi \mathbf{y}\|_{\mathbf{D}_\pi} \leq \|\mathbf{y}\|_{\mathbf{D}_\pi}^2. \quad (9)$$

774 Substituting this back yields:

$$775 \quad \mathbf{x}^\top \tilde{\mathbf{A}} \mathbf{x} \leq (\gamma - 1) \|\mathbf{y}\|_{\mathbf{D}_\pi}^2. \quad (10)$$

776 Since  $\gamma < 1$ , the quadratic form is strictly negative. Thus  $\tilde{\mathbf{A}}$  is negative definite (and consequently  
 777 Hurwitz).  
 778

779 **Step 2: Stability with  $\eta > 0$ .** The system matrix of the ODE is  $\tilde{\mathbf{A}}_\eta = \mathbf{K}\tilde{\mathbf{A}}$ . We analyze its  
 780 spectrum via a similarity transformation. Consider  $\mathbf{S} = \mathbf{K}^{-1/2}\tilde{\mathbf{A}}_\eta \mathbf{K}^{1/2}$ . Substituting  $\tilde{\mathbf{A}}_\eta = \mathbf{K}\tilde{\mathbf{A}}$ ,  
 781 we obtain:

$$782 \quad \mathbf{S} = \mathbf{K}^{-1/2}(\mathbf{K}\tilde{\mathbf{A}})\mathbf{K}^{1/2} = \mathbf{K}^{1/2}\tilde{\mathbf{A}}\mathbf{K}^{1/2}. \quad (11)$$

783 We examine the definiteness of  $\mathbf{S}$ . For any non-zero vector  $\mathbf{u}$ :

$$784 \quad \mathbf{u}^\top \mathbf{S} \mathbf{u} = \mathbf{u}^\top \mathbf{K}^{1/2} \tilde{\mathbf{A}} \mathbf{K}^{1/2} \mathbf{u}. \quad (12)$$

785 Let  $\mathbf{v} = \mathbf{K}^{1/2}\mathbf{u}$ . Since  $\eta > 0$ ,  $\mathbf{K}$  is positive definite, implying  $\mathbf{v} \neq \mathbf{0}$ . The expression simplifies to  
 786  $\mathbf{v}^\top \tilde{\mathbf{A}} \mathbf{v}$ . From Step 1, we know  $\mathbf{v}^\top \tilde{\mathbf{A}} \mathbf{v} < 0$ . Therefore,  $\mathbf{u}^\top \mathbf{S} \mathbf{u} < 0$ , meaning  $\mathbf{S}$  is negative definite.  
 787

788 Since  $\mathbf{S}$  is negative definite, all its eigenvalues have strictly negative real parts. Because  $\tilde{\mathbf{A}}_\eta$  is  
 789 similar to  $\mathbf{S}$ , they share the same eigenvalues. Thus,  $\tilde{\mathbf{A}}_\eta$  is Hurwitz. By standard stochastic approx-  
 790 imation theory (Borkar, 2008), the iteration converges globally to the unique fixed point  $\tilde{\mathbf{w}}^*$ .  $\square$   
 791

792  
 793  
 794  
 795  
 796  
 797  
 798  
 799  
 800  
 801  
 802  
 803  
 804  
 805  
 806  
 807  
 808  
 809